Modeling competition among autoreactive CD8^{+} T cells in autoimmune diabetes: implications for antigen-specific therapy

Athanasius F. M. Marée[1,3], **Pere Santamaria**[2] and **Leah Edelstein-Keshet**[1]

[1]Department of Mathematics and Institute of Applied Mathematics, University of British Columbia, 1984 Mathematics Road, Vancouver, British Columbia, V6T 1Z2, Canada
[2]Department of Microbiology and Infectious Diseases and Julia McFarlane Diabetes Research Centre, Faculty of Medicine, University of Calgary, 3330 Hospital Drive NW, Calgary, Alberta, T2N 4N1, Canada

[3]Present address: Theoretical Biology/Bioinformatics, Utrecht University, Paddualaan 8, 3584 CH Utrecht, the Netherlands

Abstract

Antigen therapy remains a promising strategy for prevention and treatment of autoimmune diseases, but translating this strategy to clinical therapy has been largely unsuccessful. We have shown that development of autoimmune diabetes in non-obese diabetic (NOD) mice involves prevalent recruitment of CD8+ T cells recognizing epitopes of islet-specific glucose-6-phosphatase catalytic subunit-related protein (IGRP). Administration of peptide analogs of IGRP206-214, the dominant epitope, reduced disease incidence but only under conditions that led to selective deletion of high-avidity T-cell clones. Peptide types or doses that resulted in elimination of all IGRP206-214-reactive T cells, regardless of avidity, promoted the recruitment of sub-dominant epitope-specific T cells and failed to prevent disease development. Here, we mathematically model competition of IGRP-reactive T-cell clones during spontaneous disease, and in response to peptide treatment. Based on realistic T-cell activation, proliferation and differentiation parameter values, our model shows that progression of spontaneous disease is characterized by (i) initial expansion of all IGRP206-214-reactive T-cell clones (irrespective of avidity) and (ii) slow replacement of T-cell clones recognizing peptide/MHC with low avidity by their high-avidity counterparts. This model helps understand the paradoxical outcomes of IGRP-based peptide treatment experiments. Furthermore, it predicts that slight deviations in dose or peptide affinity can lead to treatment failure or disease progression. This will occur if the treatment (i) increases the imbalance between competing IGRP206-214-reactive T-cell clones such that it favors rapid takeover of high-avidity clones or (ii) deletes all IGRP206-214-reactive clones, thereby creating a vacuum that promotes the recruitment of pathogenic sub-dominant specificities. Our data and model urge caution in the application of peptide therapy in autoimmunity.

Introduction

The administration of auto-antigens or auto-antigenic peptides is considered to be a promising strategy for modulating immune response in autoimmune diseases, occasionally leading to tolerance and cure (1). Despite successes in experimental animal models (2–4), human trials have generally resulted in failure (5, 6). Furthermore, in certain experimental models, peptide therapy was found to be ineffective or even counterproductive (7), promoting, rather than blunting, CTL responses against self (8). These failures indicate that the

principles on which antigen-specific therapy is based remain ill defined.

Spontaneous human autoimmune diseases result from complex immunological responses that involve T cells recognizing multiple antigenic specificities. In addition, T-lymphocyte clones reactive to individual auto-antigenic epitopes come in a wide range of ligand-binding avidities (9), and in at least some cases, avidity correlates with pathogenicity (10). Because the quality and quantity of T-cell responses are both a function

of avidity, the choice of antigen, dose, schedule of treatment and type of administration are all expected to have an important influence on the outcome of antigen therapy. All these contributing influences, however, are poorly understood and difficult to study in isolation, particularly in the context of immunologically complex autoimmune disorders.

Type 1 diabetes (T1D) is an autoimmune disease that results from killing of pancreatic β cells by autoreactive T lymphocytes. While the recruitment of autoreactive CD4$^+$ T cells is required for its initiation, compelling evidence points to an important role for CD8$^+$ T cells in initiation and/or progression of the disease. Work by us and others has provided a wealth of experimental data on the kinetic evolution of autoimmune diabetes in non-obese diabetic (NOD) mice (11). In this animal model, overt clinical disease is preceded by increases in the circulating pool (12) and avidity (9) of a prevalent population of autoreactive CD8$^+$ T cells. This sub-population, implicated as a major (albeit not exclusive) effector of β-cell destruction (13), is characterized by its ability to recognize a series of peptide analogs derived from the amino acid sequence KYNKANWFL (also known as NRP) (14). These peptides are structural and functional mimics (henceforth named mimotopes) of residues 206–214 of islet-specific glucose-6-phosphatase catalytic subunit-related protein (IGRP), a dominant β-cell auto-antigen (15).

Whereas mimotopes administered in the absence of adjuvant tend to induce deletional or functional tolerance of antigen-specific T cells *in vivo* (16, 17), recent studies have shown that the effects of NRP/IGRP-based peptide treatment on spontaneous anti-IGRP responses and diabetogenesis are complex and paradoxical (9, 18). Here, we aim to elucidate the reasons for the different outcomes that were observed, and to understand how relatively small differences in dose and peptide affinity can so dramatically affect treatment outcome. We subject available data on T-cell avidity maturation in T1D to mathematical modeling and use the model to investigate the paradoxical non-linear outcome of NRP/IGRP206-214-based peptide therapy.

Methods

Experimental methods

The experiments on T-cell avidity maturation and peptide therapy on which our model is based are described in (9, 18). Experimentally, avidity of T cells for specific peptide–MHC complexes is measured with peptide–MHC tetramers, multimeric complexes of peptide–MHC labeled with a fluorescent marker (19).

Mathematical models

The model uses data and observations specific for NOD mice, supplemented by reasonable assumptions. Parameter estimates are based on our own experiments and on the literature. We use ordinary differential equations (ODEs) to model the continuous changes in cell populations and peptide–MHC levels. The model is analyzed by common methods of non-linear dynamics and simulated numerically.

Software

Steady-state analysis, phase-space analysis and numerical integration of the model were carried out using the public domain software package GRIND (http://theory.bio.uu.nl/rdb/software.html). Contour plots of Fig. 4 were generated using the mathematical software package MAPLE (http://www.maplesoft.com/).

Results

Background

The following general background is important for assembling our model and is presented here for completeness. We assume that the naive T-cell precursors of the CTLs undergo activation in the pancreatic lymph nodes in response to auto-antigen-loaded antigen-presenting cells (APCs), most likely mature dendritic cells (20, 21). Individual T-cell clones within this sub-population bear distinct TCRs capable of recognizing antigen peptides presented by the MHC class I molecule H-2K^d (9). T cells bind to regions of APCs that present sufficiently many specific peptide–MHC complexes. Henceforth, we refer to such regions as 'sites'. Activation of the T cell occurs when sufficiently many TCRs are triggered during the contact time between the T cell and APC. Out of the thousands of diverse peptide–MHC complexes presented on the surface of an APC, ~100 complexes of a given peptide bound to a specific MHC molecule suffice to activate a T cell, by virtue of their ability to induce serial triggering of TCRs on the T-cell surface (22) [see Goldstein *et al.* (23) for a recent overview of models describing the serial triggering process]. The affinity of these TCRs for peptide–MHC, the duration of binding and the number of TCRs triggered influence whether activation occurs (24–27).

When activated, T cells proliferate and differentiate; up to ~95% of the progeny become terminally differentiated CTLs and ~5% become memory cells (28). The binding of a TCR to a peptide–MHC complex is reversible, and we refer to specific association and dissociation rates by k_{on} ($\mu M^{-1} s^{-1}$) and k_{off} (s^{-1}), respectively. The ratio $1/K_D = k_{on}/k_{off}$ is the affinity of the TCR for the given peptide–MHC complex. For a T cell, actual binding kinetics to multiple individual peptide–MHC complexes presented on an APC depend not only on the single molecular affinities but also on the number of TCRs expressed on the T cell, and the level of presentation on the APC. We use the term 'avidity' to describe the strength of association of the T cell as a whole.

In our experimental work, we have previously shown that autoimmune inflammation is associated with T-cell avidity maturation, that is, a progressive increase in the average avidity with which populations of epitope-specific CD8$^+$ T cells engage peptide–MHC. This process is associated with and accounts, in part, for the progression of benign islet inflammation to overt diabetes in NOD mice (9). We have also shown that avidity maturation of IGRP206-214-reactive CD8$^+$ T cells can be accounted for by slow amplification of a small pool of high-avidity T-cell clones at the expense of a much bigger pool of low-avidity clones (9, 10). One of the most puzzling characteristics of this avidity maturation process is that it takes place on a much longer time-scale than T-cell proliferation. Understanding this discrepancy in time-scales is one of the aims of our paper.

We have recently tested the ability of NRP/IGRP206-214-based mimotopes to protect pre-diabetic NOD mice from

developing overt T1D. The most striking observation in these studies was that the outcome of peptide therapy had a complex dependence on both the dose and type of mimotope. We use the words 'affinity of the peptide' to refer to the binding strength of the peptide–MHC complex with the TCR of the IGRP206-214-reactive T cells. Peptides with lower affinity, for example, NRP-I4, were protective in a dose-dependent manner, whereas those of higher affinity, such as NRP-V7, were ineffective. In general, therapeutic potential was negative for low peptide dose or affinity, positive for an intermediate dose or affinity and minor for high dose or affinity (18). We proposed that the protective effect requires deletion of high-avidity T-cell clones and increased recruitment of low-avidity (and potentially anti-diabetogenic) clones. In contrast, complete deletion of the prevalent IGRP206-214-reactive T-cell pool was not protective, presumably because it allowed sub-dominant epitope-specific T-cell specificities to fill the T-cell niche emptied by peptide treatment. Elucidating how peptide therapy can change the dynamics and T-cell competition is another aim of our paper.

Mathematical model of avidity maturation under peptide therapy

The goals of the model are (i) to elucidate the mechanism, time-scales and nature of the process of avidity maturation, (ii) to expose the influence of peptide dose and affinity on the outcome of peptide therapy and (iii) to outline in a quantitative context the novel philosophy proposed in (18) for peptide therapy.

Let $X_i(t)$ represent the total number of naive and memory CD8$^+$ T cells of clone i that are not bound to APCs, and let $X_{bi}(t)$ be those bound to sites on APCs. The number of terminally differentiated effector T cells of this clone is denoted as $X_{ei}(t)$. Relevant naive and memory T cells are T cells that

(i) recognize the epitope targeted by the dominant T-cell response, that is, respond to the peptide (e.g. NRP-V7) and (ii) have the potential to proliferate. All clones with a similar avidity for the given peptide are lumped together in each variable.

The dynamics of T-cell expansion depends on influx, decay and proliferation rates of the T cells, as shown in Fig. 1. The equations of our model for clone $i = 1, 2, \ldots N$ are as follows:

$$\frac{dX_i}{dt} = \sigma_i + (R_i(p) + 1)b_{off}X_{bi} - b_{on}s_fX_i - X_i\left(\delta + \varepsilon\sum_{j=1}^{N}X_j\right), \quad (1a)$$

$$\frac{dX_{bi}}{dt} = b_{on}s_fX_i - b_{off}X_{bi}, \quad (1b)$$

$$\frac{dX_{ei}}{dt} = R_{ei}(p)b_{off}X_{bi} - \delta_eX_{ei}. \quad (1c)$$

Here, σ_i, the influx of naive clone i T-cells from the thymus, and δ, the turnover of lymphocytes, are assumed constant. Growth of clones occurs within a limited lymphocyte pool size (29), and ε represents the level of competition for that pool. We assume that δ and ε are roughly the same for all lymphocyte clones, since otherwise competitive exclusion (30) would always select the same favored clone, undermining the diversity of the adaptive immune system. $R_i(p)$ and $R_{ei}(p)$ are proliferation rates that are ultimately dependent on endogenous and administered peptide levels via MHC loads (see below.)

T cells proliferate only after the appropriate signal from APCs. Several sources (31–33) show that T cells compete for sites on APCs. For s_f, the number of free sites on APCs, the rates of binding (b_{on}) and unbinding (b_{off}) of T cells to these sites are assumed constant, whereas memory cell formation is depicted by the term R_i. Similarly, the proliferation of naive and memory T cells into effectors is depicted by the function R_{ei},
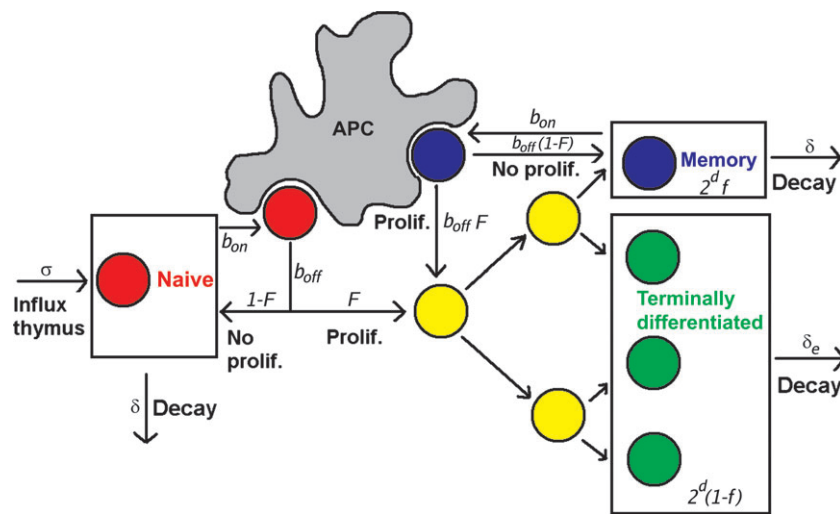

Fig. 1. Scheme of the model showing the main classes of CD8$^+$ T cells (of a given clone) considered. The free naive and memory T cells (X_i) become bound (X_{bi}) to an APC. This potentially leads to proliferation into both terminally differentiated CTLs (X_{ei}) and memory T cells. Proliferating T cells that produce more than a single memory cell contribute to clonal expansion. The meanings and values of the parameters indicated in the figure are given in Table 1.

whereas the decay rate of such effector cells, δ_e, is assumed constant.

The population of terminally differentiated effector T cells does not proliferate and does not compete for selection, but as these form the bulk of cells measured in experiments, their role in the development of diabetes is crucial. Turnover rates of effector cells are much greater than those of naive T cells: their growth rate is 20 times larger and their half-life is only 3 days (34–36). For the effector cells, homeostatic competition terms can therefore be ignored.

In order to close the system, we must specify the number of free sites on APCs as well as the details of the proliferation and differentiation rates. Let s stand for the total number of sites recognized by the relevant T-cell clones (on all APCs), assumed constant. Then the number of free sites available for binding is simply

$$s_f = s - \sum_i X_{bi}. \tag{2}$$

Proliferating T cells produce a large number of terminally differentiated effector cells and a small number of memory cells for self-renewal (37). Following peptide therapy, a huge T-cell expansion is observed, followed by decay to a much lower level within a few weeks (our unpublished results). Experimental evidence (38, 39) suggests that T-cell deletion at high peptide dose is due to clonal exhaustion, that is, to the fact that not enough memory cells are produced for self-renewal. Only ~5% of the progeny of proliferating T cells are memory cells (40), and at high levels of peptide presentation, this memory cell production decreases (41, 42), accounting for the observed clonal exhaustion.

We use M_i and E_i to denote the number of memory and effector cells produced per proliferating T cell. Memory cells in excess of simple replacement, $(M_i - 1)$, contribute to 'expansion' of a clone. Let F_i stand for the fraction of clone i T-cells activated after leaving an APC. Combining proliferation and memory cell production, the expansion factors R_i and R_{ei} for clone i are then given by

$$R_i = F_i(M_i - 1), \quad R_{ei} = F_i E_i. \tag{3}$$

The quantities F_i, M_i and E_i depend on the level of peptide-MHC presentation at sites on APCs, and this, in turn, depends on native and administered peptides.

Whether a T cell bound to an APC will proliferate or not, depends on the number of peptide–MHC complexes at the given site (32) and the affinity of the TCRs for the peptide (43). We take proliferation to be a saturating sigmoidal function of the 'MHC load', m_t (i.e. the effective number of peptide–MHC complexes per APC site that can trigger a given TCR, taking both the level of presentation and the potential of the peptides to trigger TCRs into account):

$$F_i = \frac{m_t^2}{a_i^2 + m_t^2}, \tag{4}$$

where a_i is the MHC level at which half of the i-type T cells become activated.

A proliferating T cell goes through a number, d, of cell divisions, producing 2^d daughter cells. Of these, we assume that a fraction f are memory cells and $(1 - f)$ are effector cells, where f depends on the level of presentation. We assume that the number of memory cells, M_i, produced per proliferating i-type T cell has a Hill-function dependence on the MHC level. Thus,

$$E_i = 2^d(1 - f), \tag{5a}$$

$$M_i = 2^d f, \tag{5b}$$

$$\text{where} \quad f = r\left(1 - \frac{m_t^n}{(h + a_i)^n + m_t^n}\right). \tag{5c}$$

Here r gives the maximal fraction of memory cells produced; $(h + a_i)$ is the MHC level for half-maximal memory cell production (h describes the increase of MHC level needed to shift the T-cell dynamics from expansion to clonal exhaustion). The Hill coefficient $n = 3$ best represents experimental observations.

Given the above dependencies on MHC load, we want to estimate the level of presentation of peptide–MHC complexes per site resulting from peptide therapy with mimotopes of type j. Let p_j denote the amount of mimotope of type j that is not bound to any MHC, and p_{jb} denote the amount of mimotope that is bound to MHCs at a specific site. Since only a tiny proportion of the peptides become bound to MHC molecules, p_j is approximately equal to the total amount of j-type mimotope, and we refer to it as the 'dose'. Let e_j denote the efficacy of mimotope j (relative to endogenous peptide) to trigger TCRs. Then by effective MHC load, m_t, we mean the sum of peptide 'doses' weighted by their relative TCR triggering efficacy,

$$m_t = \sum_j e_j p_{jb}. \tag{6}$$

The sum of all peptides presented is $\sum_j p_{jb}$. Denoting by m, m_f the total and the free MHC molecules per site, we have $m = m_f + \sum_j p_{jb}$. By simple mass action,

$$\frac{dp_{jb}}{dt} = k_{on_p} p_j m_f - k_{off_p} p_{jb}, \tag{7}$$

where k_{on_p} is the binding rate of peptides to MHC molecules, and k_{off_p} combines the unbinding rate of the peptide from the MHC with the turnover rate of the peptide–MHC complex itself. Both rates are assumed to be the same for all peptides. The values e_j (on an arbitrary scale) rank the relative potency of the various peptides in the context of TCR triggering. Generally, we chose a scaling for the weights so that an endogenous peptide is represented by TCR triggering efficacy $e_0 = 1$, and the single mimotope is then associated with a weight $e_1 = e$ relative to this. The above summarizes the scheme of our model in a general setting of N T-cell clones. Before analyzing its behavior, we simplify the model to consider a case leading to maximal insights within the simplest realistic setting.

The simplified two-clone model

In this section, we introduce several simplifying assumptions to fully expose the key features of T-cell competition leading to avidity maturation. First, in view of the rapid time-scale of peptide processing relative to T-cell population dynamics, we consider peptide bound to MHC to be at quasi-steady state (QSS) ($dp_{bi}/dt \approx 0$). Further, we consider just two peptides, with p_0 the level of endogenous self-antigen and p_1 the administered mimotope, whose relative TCR triggering efficacy is e. Then,

$$p_{0b} = \frac{mp_0}{\sum_i p_i + \frac{k_{off_p}}{k_{on_p}}}, \quad p_{1b} = \frac{mp_1}{\sum_i p_i + \frac{k_{off_p}}{k_{on_p}}}, \quad (8)$$

and the effective MHC load is $m_t = p_{0b} + ep_{1b}$, so

$$m_t = \frac{(p_0 + ep_1)m}{p_0 + p_1 + c}, \quad (9)$$

where c represents other background ligands plus the ratio (k_{off_p}/k_{on_p}). This expression is reasonable: it incorporates increased effective MHC presentation level as the peptide dose p_1 increases (provided the TCR triggering efficacy of the peptide, e, is adequate), but it also includes the effect of peptide competition. The outcome depends on both dose, p_1, and relative TCR triggering efficacy, e, of the mimotope in comparison with the level and efficacy of endogenous peptide.

To investigate the key features of avidity maturation under peptide therapy, it suffices to consider the interactions of two avidity types of CD8$^+$ T cells and follow relative prevalence of these clones. We thus follow two clones, with $X = X_1$ and $Y = X_2$, respectively, the low- and high-avidity clones. (Subscripts are dropped in the next section, to ease notation.) We further assume that bound cells are at QSS with free cells:

$$\frac{dX_{bi}}{dt} = b_{on}s_fX_i - b_{off}X_{bi} \approx 0, \quad i = 1, 2. \quad (10)$$

Then $X_{b1}/X_{b2} = X_1/X_2$, and we obtain:

$$X_{bi} = \frac{sX_i}{X_1 + X_2 + \frac{b_{off}}{b_{on}}}, \quad i = 1, 2. \quad (11)$$

The effect of constant background T-cell clones competing for other presented peptides at the same sites can be assimilated into the parameter b_{on}. With these assumptions, the equations for free naive and memory T cells of clone i are

$$\frac{dX_i}{dt} = \sigma_i + R_i b_{off} \frac{sX_i}{X_1 + X_2 + \frac{b_{off}}{b_{on}}}$$
$$- \delta X_i - \varepsilon X_i(X_1 + X_2), \quad i = 1, 2. \quad (12)$$

(Note that due to the QSS assumption of Eqs. 10, two terms have dropped out.) The constants σ_i, b_{off} and ε are as before, and R_i are proliferation rates as given in Eq. 3. The background competition with other sub-dominant clones is now incorporated into the constant δ.

Once these equations are solved, the effector T-cell population levels can be determined from the equations

$$\frac{dX_{ei}}{dt} = R_{ei}b_{off} \frac{sX_i}{X_1 + X_2 + \frac{b_{off}}{b_{on}}} - \delta_e X_{ei}, \quad i = 1, 2. \quad (13)$$

To summarize, the model consists of two ODEs (Eqs. 12, i = 1, 2) for the naive and memory cells of the two T-cell clone types, with parameters given by the expansion factors (Eqs. 3, 4 and 5b), and MHC level (Eq. 9). Solving these equations then leads to a pair of subsidiary ODEs (Eqs. 13) for the effector T cells that can, in turn, be solved or simulated.

Clonal competition and the effect of peptide therapy

To simplify notation, from here on we write $X = X_1$ for the low-avidity clone and $Y = X_2$ for the high-avidity clone. Detailed consideration of experimental data for NOD mice allows us to validate the model in a quantitatively meaningful context, using realistic parameter values (default values shown in Table 1). T-cell abundance is always expressed as the total number of cells per animal. The initial virgin state is given by $X = \sigma_x/\delta = 900$ and $Y = \sigma_y/\delta = 100$, and dynamics are simulated for 168 days (24 weeks). Simulations of the model predict the following trends:

(1) Both types of T cells expand rapidly over the first 6 weeks, maintaining near-constant proportion (see the initially linear part of the trajectory in the (X, Y) phase plane of Fig. 2A). The initial expansion phase is characterized by weak competition. The larger influx of T cells with low avidity causes initial dominance of these low-avidity cells.

(2) Competition and differential expansion result in slight advantage of clone Y, which slowly overtakes and re-places X after ~20 weeks (Fig. 2B). The long time-scale is due to slow replacement of the different clones within the memory pool, as well as strong competition for sites on APCs during the later stages. These later stages are critically affected by peptide therapy. The number of non-pathogenic (X_e) and highly pathogenic (Y_e) effector T cells have similar profiles, and closely follow the dynamics observed in the populations of naive and memory T cells (Fig. 2C). Slow replacement by the high-avidity clones agrees well with the experimental data (9).

(3) The model predicts vastly different possible outcomes for peptide therapy, in agreement with observed paradoxical results (18). Figure 3 demonstrates the effect of the dose of a single mimotope recognized (in the context of MHC) with intermediate affinity by TCRs on cognate T cells. Figure 3A shows that when this intermediate affinity peptide is administered at low doses, the high-avidity clones expand more rapidly; when given at moderate doses, these high-avidity clones are deleted, whereas the low avidity ones expand and when given at high doses, the ratios of high- to low-avidity clones hardly change. This also agrees with experimental results of Han *et al.* (18). Figure 3B indicates that overall expansion occurs at low and moderate peptide doses. While at low doses, the high-avidity clones dominate, leading to accelerated disease progression, and at moderate doses, low-avidity

Table 1. Parameter values used in the model

Parameters	Meaning	Value units	Reference
σ_x	Influx of low-avidity T cells from the thymus	9 cell day^{-1}	(49)[a]
σ_y	Influx of high-avidity T cells from the thymus	1 cell day^{-1}	(49)[a]
δ	Death rate of naive and memory T cells	0.01 day^{-1}	(34, 35)[b]
δ_e	Death rate of effector T cells	0.3 day^{-1}	(36)[b]
ε	Homeostasis of T-cell pool	10^{-6} cell day^{-1}	[c]
b_{off}	Unbinding rate of T cell from APC	6 day^{-1}	(50)[d]
b_{on}	Binding rate of T cell to APC	5×10^{-4} day^{-1}	[c]
d	Number of cell divisions per proliferating T cell	6	(26, 40, 51)
r	Maximal fraction of daughter cells that are memory cells	0.05	(40, 51)
s	Total number of binding sites on APCs	20 000	[e]
a_x	MHC level at which half of the low-avidity T cells become activated	130 MHC/site	[f]
a_y	MHC level at which half of the high-avidity T cells become activated	120 MHC/site	[f]
h	Increase of MHC level needed to shift the T-cell dynamics from expansion to clonal exhaustion	80 MHC/site	[f]
m	Maximum number of MHC complexes per site	1000 MHC/site	[f]
c	Peptide level for half-maximal MHC binding	245 μg	[g]
p_0	Amount of endogenous peptide	5 μg	[g]
p_1	Amount of injected mimotope	0–100 μg	[g]
e	Relative TCR triggering efficacy of mimotope	0–1.5	[h]

[a]The mouse lymphocyte repertoire consists of ~10^8 lymphocytes (49). Given a turnover of 1% day^{-1} (34), the influx of T cells from the thymus is ~10^6 day^{-1}. The total number of T-cell clones in mice is ~10^7 (49), so every clone is produced once per 10 days. Suppose that 100 clones recognize the peptide at a level high enough to trigger their own proliferation, then the daily influx should be ~10. Assuming that 90% of these naive T cells have low avidity, we estimate $\sigma_x = 9$ and $\sigma_y = 1$. [b]The lifespan of naive and memory T cells is ~100 days (34, 35), while for effector T cells, it is roughly 3 days (36). [c]The parameters ε and b_{on} have been used to adjust the dynamics of the model. [d]T cells and APCs form an immunological synapse that lasts for ~4 h. [e]Each pancreatic lymph nodes (PLNs) contains ~10^6 cells, 1% of which are APCs. With ±4 PLNs per mice and at most around five T cells concurrently binding to the same APC, the total number of sites is ~2 × 10^5. We here assume that only 10% of those sites present the peptide at a sufficiently high level to establish an immunological synapse. [f]We are currently working on better estimates, based on the kinetics of the MHC peptide–TCR complex and a detailed description of the TCR down-regulation by serial engagement. [g]With these choices of parameter values for p_0 and c, 20 peptide–MHC complexes are initially presented. Varying the parameter p_1 from 0 to 100 μg, leads to an increase in peptide presentation from 20 to 300; this alters the dynamics from expansion to clonal exhaustion. Unless otherwise indicated, we chose $p_1 = 100$ μg in our simulations. [h]A direct link between the affinity of a mimotope and this parameter is not currently available. In the simulations, we used $e = 1$, unless otherwise indicated.

clones grow and overtake their pathogenic, high-avidity counterparts, leading to disease protection. At high doses, deletion of all T-cell clones (high and low avidity) creates a 'niche' for other clones [likely sub-dominant, see Han *et al.* (18)]. Now these can expand and dominate, fostering disease progression. The model predicts a large T-cell expansion in the first 3 weeks of high-dose therapy (Fig. 2D), which agrees well with our own unpublished results.

(4) The model shows that a delicate balance between peptide dose and affinity is needed to promote the recruitment of the 'protective' (type *X*) T cells (protective here denotes blocking high-avidity clones from gaining dominance, but we do not exclude other possible forms of active protection). This delicate balance is reflected in Fig. 4A. The figure plots the predicted abundance of low- (green) and high (red)-avidity T cells after 24 weeks of treatment for 15 000 different peptide therapy regimes administered regularly and continuously (see Discussion of other forms of administration further on). The time course of therapy is generally as follows: after ~3 weeks of peptide treatment, there is a rapid shift in the proportions of low- and high-avidity clones (see Fig. 2D) and a strong effect of therapy is observed. (The time-scale depends partly on what is assumed to be the 'protective threshold'.) A second, longer phase, then results in complete dominance of one or the other T-cell clone. We varied both the dose, p_1, and the relative TCR triggering efficacy, e, of the mimotope to

show the array of possible peptide effects. Note that the distribution of therapy strategies (p_1 and e) that lead to recruitment of the greatest number of protective, low-avidity clones (highest ridge on the green surface) is non-linear. Slight departures from these strategies can result in dominance of pathogenic, high-avidity clones (highest ridge on the red surface). The delicate balance also means that the timing of therapy is critical, as the dynamics are sensitive to initial conditions: If therapy is started too late, the tendency of high-avidity clones to dominate would be already strong, and thus, much harder to reverse (see Fig. 2A). This emphasizes the idea that achieving an optimal balance between peptide dose and TCR triggering efficacy (as well as the timing of the therapy) is of paramount importance in the effectiveness of peptide therapy.

(5) Effector T cells have high turnover, and closely track the dynamics of the naive and memory populations. We compared the dynamics of the full model with those in which a QSS approximation was made ($dX_e/dt = dY_e/dt \approx 0$) and found close agreement, except during the transient phase in the first weeks after treatment initiation (see Fig. 5B). This suggests that for understanding and predicting long-term dynamics of clonal competition, the CTLs can be ignored. Moreover, after the first 3 weeks of peptide therapy (but not before), the observed relative abundances of different T-cell clones (e.g. the ratio X/Y or X_e/Y_e) should be good indicators of the state of competition.
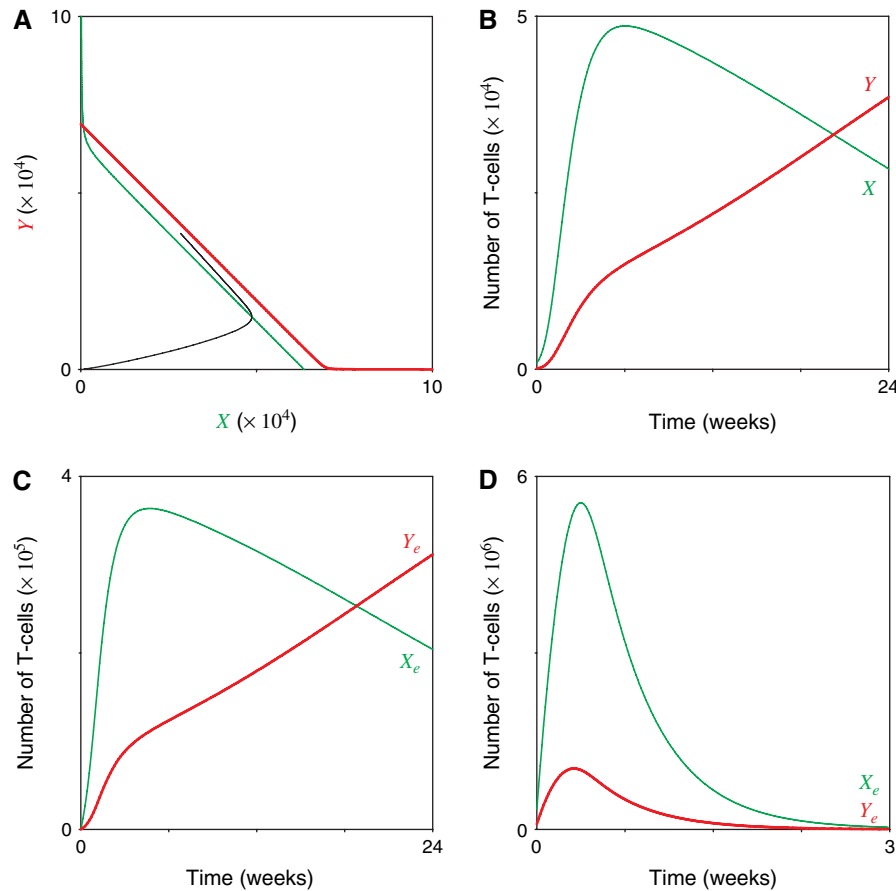
Fig. 2. (A) After fast expansion of both populations, the low-avidity T cells are slowly replaced by high-avidity T cells, as shown in this (*X*, *Y*) phase plane for the two-clone model (Eqs. 12, *X* = low-avidity clone population, *Y* = high-avidity clone population; thin line: *X* nullcline; thick line: *Y* nullcline). A single trajectory, starting in the virgin state close to the origin and corresponding to the dynamics shown in *B* is superimposed. After an initial 'detour' into the positive (*X*, *Y*) plane, the trajectory heads toward a steady state in which *Y* dominates and *X* has a very low (but non-zero) level. In (B–D), *X* = thin curve and *Y* = thick curve. (B) Time-plot of the model, showing the number of low- (*X*) and high (*Y*)-avidity T cells, given by Eqs. 12, over a period of 24 weeks. (C) Time-plot of the resulting dynamics of the effector populations (*X_e* and *Y_e*) given by Eqs. 13. (D) Time-plot of the model showing the levels of the effector T-cell populations over a period of 3 weeks after a high-dose peptide therapy is started (therapy is started at 3 weeks of age). A temporary huge expansion can be observed over the first week.

(6) We further investigated the possibility that peptide therapy not only affects the number of MHCs per APC that present the peptide but also the number of APCs that do so. Figure 4B shows the level of low- (green) and high (red)-avidity T cells after 24 weeks of treatment for different combinations of both variables. Increasing the number of APCs accelerates avidity maturation due to decreasing time intervals between successive activation and proliferation steps, while increasing the number of MHC per APC blunts avidity maturation due to the fact that the difference in activation and proliferation rate between high- and low-avidity clones becomes small. Both effects are expected to occur simultaneously during peptide therapy, making experimental outcomes even more unpredictable.

Discussion

We have constructed a quantitative mathematical model for T-cell competition dynamics in T1D to investigate whether and how treatment with mimotopes specific for a prevalent population of autoreactive T cells in NOD mice can bring about prolonged protection from T1D. As inputs to this model, we used known features of the immune system and parameters based on experimental data. As outputs, we used the model to study the naive versus activated state, the level of memory versus effector T cells, the influence of peptide dose and avidity on treatment efficacy and the relative roles of pro-liferation and clonal exhaustion in T-cell avidity maturation and in response to peptide therapy. The dynamics of autoimmune disease progression in both untreated and peptide-treated mice are well explained by a process of clonal competition of non-pathogenic (low avidity, *X*) and pathogenic (high avidity, *Y*) clones. We found two distinct phases, with different time-scales, of T-cell avidity maturation during T1D progression: an initial stage characterized by rapid expansion of all relevant T cells, with more or less constant proportions of different clones, and a later stage in which the *Y* clone, with its larger expansion factor, R_y, outcompetes others and takes over.
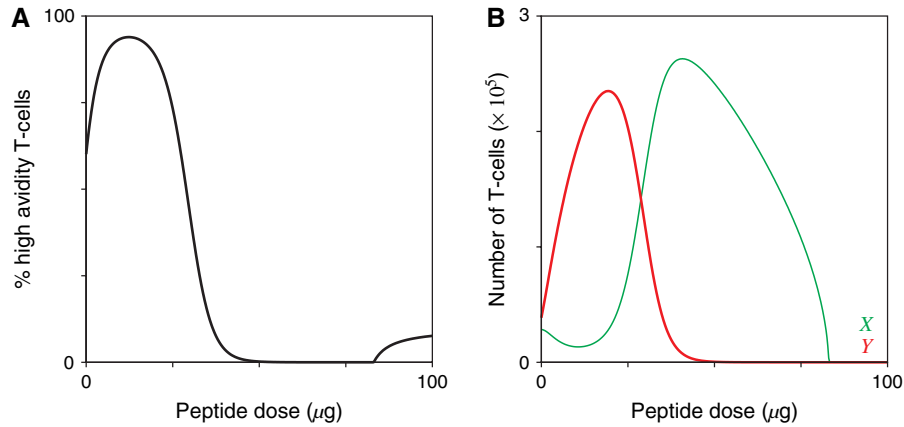
Fig. 3. (A) Percentage high-avidity (type *Y*) T cells after 24 weeks versus peptide dose, p_1. An intermediate dose (40–70 μg) has the best therapeutic potential, whereas a low dose (15–25 μg) leads to a higher fraction of high-avidity T cells, and would hence accelerate the pathology. (B) Total number of low- (*X*) and high (*Y*)-avidity T cells after 24 weeks versus peptide dose. The low-avidity cells dominate at the dose range 40–80 μg; at higher doses, all clones are deleted, creating space for other T-cell populations to take over.

Another output of the model is the prediction of the population-level response to systemic treatment with different mimotopes. The model describes how T-cell activation, proliferation and differentiation are affected by peptide dose and/or affinity. Thus, it provides an understanding of the mechanisms underlying the paradoxical non-linear outcome of NRP/IGRP206-214-based peptide therapy (18). Specifically, it shows how dynamics at the level of individual T-cell clones can result in avidity maturation of the entire population of clones targeting a single antigenic epitope. It also illustrates why manipulation of clonal competition for dominance using mimotopes is a double-edge sword: treatment can lead to protection when it fosters the expansion and recruitment of low-avidity (non-pathogenic) clones but it can also accelerate disease if it promotes the expansion of high-avidity clones or the recruitment of other (sub-dominant yet pathogenic) populations of autoreactive T cells. Thus, success of peptide therapy hinges on an optimal balance between dose and affinity, and slight departures from this balance may be ineffective or even harmful.

Our model is based on continuously administered mimotopes. Response to a single injection or to a discrete number of injections would be much more difficult to quantify, requiring many more assumptions about pharmaceutical kinetics of the absorption, presentation and clearance. In principle, the correctly designed dose and affinity of a single mimotope injection should delay the disease, just as the wrong design choice could accelerate it. Keeping track of the changing level of circulating and presented mimotopes is beyond the scope of our model at this point, and the complex temporal variations of peptide and its presentation between injections would introduce a sequence of regimes in which different T-cell clones expand and collapse.

In constructing and analyzing the model, we have made some simplifications and assumptions that warrant discussion. First, we assumed that the thymic output terms σ_i (with $\sigma_x \gg \sigma_y$) are not affected by peptide therapy. This assumption may not be entirely accurate. For example, in a transgenic mouse where the thymus predominantly exports intermediate to high-avidity T cells, high doses of high-affinity peptides

result in substantial thymocyte deletion (our unpublished results). Since the thymic output of specific clones is very small during the initial phase, stochastic effects are anticipated. However, influx of naive cells plays a marginal role during the slow replacement phase, when memory T cells dominate. We therefore predict that any effects of mimotopes on the thymic output terms have, at best, a minor effect on the outcome of the therapy once the immune process has progressed sufficiently, that is, if therapy begins later than 3 weeks into the adaptive immune response.

Second, we chose a competition term in the form $rX_i/(1 + X_i)$ rather than $rX_i(1 - X_i/K)$ because T cells are continuously binding to and detaching from sites on APCs (and proliferating), even at high population levels. In alternate competition models where the T-cell growth rate tends to zero as the population increases, the replacement rate would depend only on the death rate, which, in the case of naive and memory T cells, would be far too slow to account for avidity maturation.

Third, the model suggests that strong competition is occurring, that is, the estimated value of the competition parameter, ε, is quite high. Much lower values of ε lead to high variations in the total cell population during peptide therapy, because the carrying capacity then depends almost linearly on the expansion factor. Such variations, however, have not been observed experimentally. If the level of competition with unrelated clones were similarly strong, then the total level of competition would become unreasonably high. We therefore conclude that the high level of T-cell competition is due to crowding within the regional lymph nodes. This would explain why similar clones responding to the same peptide–MHC complex compete much more with one another than with unrelated clones.

Fourth, many biological processes that impact autoimmune disease were not included in this model. For example, notwithstanding the contribution of CD4^{+} T_h to CD8^{+} T-cell priming, we did not consider these cells explicitly in the model, because CD4^{+} T cells should not alter the competitive balance between high- and low-avidity epitope-specific MHC class I-restricted T cells, despite their contribution to CD8+
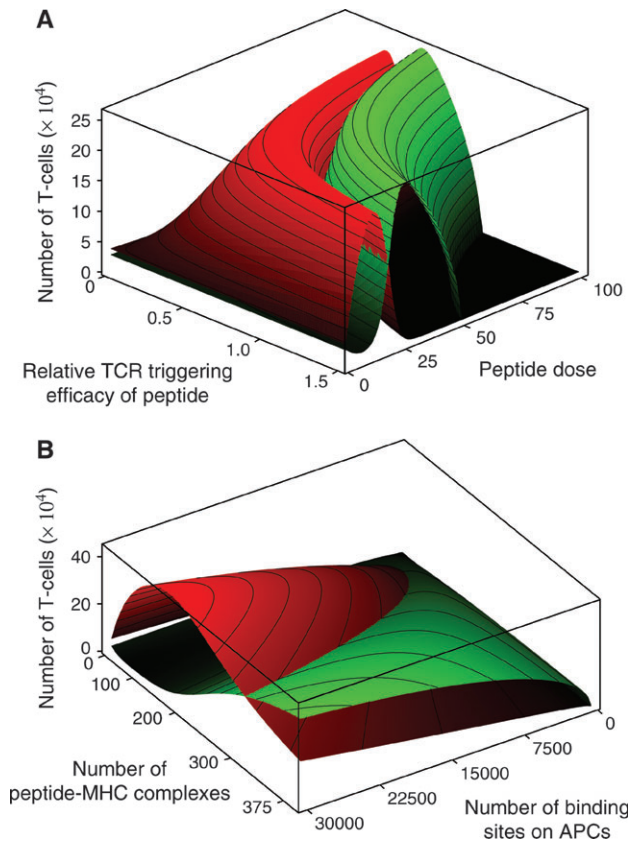
Fig. 4. (A) The combined effect of dose, p_1, and relative TCR triggering efficacy, e, of the peptide on the outcome of peptide therapy. The graph shows the population sizes of low-avidity, X (green), and high-avidity, Y (red), T cells after 24 weeks. Intermediate peptide doses, and/or relative triggering efficacy, are needed to obtain a high level of X and a low level of Y. (B) Population sizes of X (green) and Y (red) after 24 weeks for different levels of binding sites on APCs, s, and/or peptide–MHC complexes per site presenting the peptide, m_t. To emphasize the opposite effect of those two different ways in which presentation can increase, we have excluded in these simulations the variation in memory cell production, as defined by Eq. 5b. Instead, we used $M_x = M_y = 2^d r = \text{constant}$.

T-cell survival, recruitment or memory. Also, a potential increase in the level of presentation of endogenous peptide (IGRP206-214) resulting from T cell-mediated β-cell death was not considered. This feedback loop could potentially explain periodicities observed in the size of the circulating IGRP206-214-reactive T-cell pool during the pre-diabetic phase (12), and could conceivably play a role in accelerating the rate of T-cell avidity maturation.

The fifth and last potential caveat on the interpretation of our model and experimental data is that, although both strongly suggest that clonal exhaustion occurs during peptide therapy, other mechanisms could also influence and (partly) account for the observed trends. For example, (i) protective mimotopes might activate certain subsets of canonical regulatory T cells that might affect the kinetics of T-cell avidity maturation (44). For this to occur, however, these regulatory T cells would have to express mimotope-reactive TCRs (which is unlikely) or would have to undergo activation in response to cytokines, such as CD8^{+} T cell-derived IL-2 (a more realistic possibility); (ii) most likely, some fraction of the injected mimotopes will be presented by non-professional APCs (much more abundant than professional APCs). This could lead to an increased activation level and anergy, due to down-regulation of the TCR level (45) or to a reduction in the level of co-stimulatory receptors, such as CD28 (46). However, the huge expansion observed during early peptide treatment (our unpublished results) shows that this cannot be the dominant effect, and proves that the treatment causes a significant increase in presentation by professional APCs; (iii) the model can only account for observations made with agonists [full or partial as in Han *et al.* (18)], but certain mimotopes might instead have an antagonistic effect on TCR triggering (and therefore, a negative value of e). Such antagonistic effects have been observed by Bachmann *et al.* (47) and modeled by Rabinowitz *et al.* (48).

Regardless of the contribution of these alternate mechanisms, our model is consistent with and supports the interpretation of the paradoxical results of Han *et al.* (18). That is, in polyclonal autoimmune responses involving multiple epitopes in each of several auto-antigens, and T-cell clones
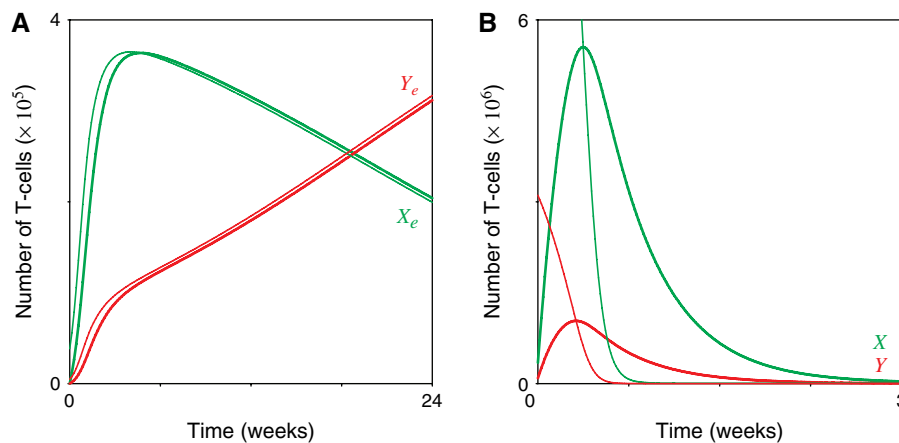

Fig. 5. (A) Time-plot of the total number of effector T cells showing the full model (thick lines) as well as results of the QSS approximation (thin lines). (*B*) Comparison of the full model (curves with a peak) and the QSS assumption (decreasing curves) for the dynamics of Fig. 2*D*. The QSS approximation is not satisfied for sudden changes, and it fails to track the transient peak in the effector T cells after initiation of peptide therapy.

recognizing each epitope with a range of avidities, the effectiveness of mono-specific peptide therapy increases when it promotes both expansion of non-pathogenic, low-avidity T cells and deletion of their high-avidity counterparts. Our model supports the idea that both processes are driven by competition between the T cells for binding to APCs and subsequent activation and proliferation in the regional lymph nodes. We predict two of the experimental outcomes that were observed. First, therapeutic effectiveness requires continued treatment. Initiation of an effective mimotope therapeutic protocol (in terms of dose and peptide affinity) at an advanced stage of the disease process delayed, but did not blunt, T1D development (18). Second, the response to peptide therapy is highly non-linear (not directly proportional to the dose or affinity of the peptide). According to the model, this is due to the fact that therapy affects both the speed of clonal replacement and the expansion factors that determine the outcome of competition. Thus, it illustrates that a delicate balance between dose and affinity of peptide is needed to elicit autoimmune disease protection.

Acknowledgements

Abbreviations

APC	antigen-presenting cell
IGRP	islet-specific glucose-6-phosphatase catalytic subunit-related protein
NOD	non-obese diabetic
NRP	amino acid sequence KYNKANWFL
ODE	ordinary differential equation
QSS	quasi-steady state
T1D	type 1 diabetes

References

1 Weiner, H. L. 1997. Oral tolerance for the treatment of autoimmune diseases. *Annu. Rev. Med.* 48:341.

2 Zhang, Z. J., Davidson, L., Eisenbarth, G., and Weiner, H. L. 1991. Suppression of diabetes in nonobese diabetic mice by oral administration of porcine insulin. *Proc. Natl Acad. Sci. USA* 88:10252.

3 Daniel, D. and Wegmann, D. R. 1996. Protection of nonobese diabetic mice from diabetes by intranasal or subcutaneous administration of insulin peptide B-(9-23). *Proc. Natl Acad. Sci. USA* 93:956.

4 Gottlieb, P. A. and Eisenbarth, G. S. 2002. Insulin-specific tolerance in diabetes. *Clin. Immunol.* 102:2.

5 Chaillous, L., Lefèvre, H., Thivolet, C. *et al.* 2000. Oral insulin administration and residual beta-cell function in recent-onset type 1 diabetes: a multicentre randomised controlled trial. Diabete Insuline Orale group. *Lancet* 356:545.

6 Diabetes Prevention Trial—Type 1 Diabetes Study Group. 2002. Effects of insulin in relatives of patients with type 1 diabetes mellitus. *N. Engl. J. Med.* 346:1685.

7 Hänninen, A. 2000. Prevention of autoimmune type 1 diabetes via mucosal tolerance: is mucosal autoantigen administration as safe and effective as it should be? *Scand. J. Immunol.* 52:217.

8 Blanas, E. and Heath, W. R. 1999. Oral administration of antigen can lead to the onset of autoimmune disease. *Int. Rev. Immunol.* 18:217.

9 Amrani, A., Verdaguer, J., Serra, P., Tafuro, S., Tan, R. and Santamaria, P. 2000. Progression of autoimmune diabetes driven by avidity maturation of a T-cell population. *Nature* 406:739.

10 Han, B., Serra, P., Yamanouchi, J. *et al.* 2005. Developmental control of CD8(+) T cell-avidity maturation in autoimmune diabetes. *J. Clin. Invest.* 115:1879.

11 Delovitch, T. L. and Singh, B. 1997. The nonobese diabetic mouse as a model of autoimmune diabetes: immune dysregulation gets the NOD. *Immunity* 7:727.

12 Trudeau, J. D., Kelly-Smith, C., Verchere, C. B. *et al.* 2003. Prediction of spontaneous autoimmune diabetes in NOD mice by quantification of autoreactive T cells in peripheral blood. *J. Clin. Invest.* 111:217.

13 Verdaguer, J., Yoon, J.-W., Anderson, B. *et al.* 1996. Acceleration of spontaneous diabetes in TCR-β-transgenic nonobese diabetic mice by β-cell cytotoxic CD8$^+$ T cells expressing identical endogenous TCR-α chains. *J. Immunol.* 157:4726.

14 Anderson, B., Park, B.-J., Verdaguer, J., Amrani, A. and Santamaria, P. 1999. Prevalent CD8$^+$ T cell response against one peptide/MHC complex in autoimmune diabetes. *Proc. Natl Acad. Sci. USA* 96:9311.

15 Lieberman, S. M., Evans, A. M., Han, B. *et al.* 2003. Identification of the β cell antigen targeted by a prevalent population of pathogenic CD8$^+$ T cells in autoimmune diabetes. *Proc. Natl Acad. Sci. USA* 100:8384.

16 Aichele, P., Kyburz, D., Ohashi, P. S. *et al.* 1994. Peptide-induced T-cell tolerance to prevent autoimmune diabetes in a transgenic mouse model. *Proc. Natl Acad. Sci. USA* 91:444.

17 Toes, R. E., Offringa, R., Blom, R. J., Melief, C. J. and Kast, W. M. 1996. Peptide vaccination can lead to enhanced tumor growth through specific T-cell tolerance induction. *Proc. Natl Acad. Sci. USA* 93:7855.

18 Han, B., Serra, P., Amrani, A. *et al.* 2005. Prevention of diabetes by manipulation of anti-IGRP autoimmunity: high efficiency of a low-affinity peptide. *Nat. Med.* 11:645.

19 Altman, J. D., Moss, P. A. H., Goulder, P. J. R. *et al.* 1996. Phenotypic analysis of antigen-specific T lymphocytes. *Science* 274:94.

20 Zhang, Y., O'Brien, B., Trudeau, J., Tan, R., Santamaria, P. and Dutz, J. P. 2002. *In situ* β cell death promotes priming of diabetogenic CD8 T lymphocytes. *J. Immunol.* 168:1466.

21 Liblau, R. S., Wong, F. S., Mars, L. T. and Santamaria, P. 2002. Autoreactive CD8 T cells in organ-specific autoimmunity: emerging targets for therapeutic intervention. *Immunity* 17:1.

22 Valitutti, S., Müller, S., Cella, M., Padovan, E. and Lanzavecchia, A. 1995. Serial triggering of many T-cell receptors by a few peptide-MHC complexes. *Nature* 375:148.

23 Goldstein, B., Faeder, J. R. and Hlavacek, W. S. 2004. Mathematical and computational models of immune-receptor signalling. *Nat. Rev. Immunol.* 4:445.

24 Viola, A. and Lanzavecchia, A. 1996. T cell activation determined by T cell receptor number and tunable thresholds. *Science* 273:104.

25 Margulies, D. H. 1997. Interactions of TCRs with MHC-peptide complexes: a quantitative basis for mechanistic models. *Curr. Opin. Immunol.* 9:390.

26 Wells, A. D., Gudmundsdottir, H. and Turka, L. A. 1997. Following the fate of individual T cells throughout activation and clonal expansion: signals from T cell receptor and CD28 differentially regulate the induction and duration of a proliferative response. *J. Clin. Invest.* 100:3173.

27 Savage, P. A., Boniface, J. J. and Davis, M. M. 1999. A kinetic basis for T cell receptor repertoire selection during an immune response. *Immunity* 10:485.

28 Sallusto, F. and Lanzavecchia, A. 2001. Exploring pathways for memory T cell generation. *J. Clin. Invest.* 108:805.

29 Freitas, A. A. and Rocha, B. 2000. Population biology of lymphocytes: the flight for survival. *Annu. Rev. Immunol.* 18:83.

30 De Boer, R. J. and Perelson, A. S. 1994. T cell repertoires and competitive exclusion. *J. Theor. Biol.* 169:375.

31 De Boer, R. J. and Perelson, A. S. 1997. Competitive control of the self-renewing T cell repertoire. *Int. Immunol.* 9:779.

32 Borghans, J. A. M., Taams, L. S., Wauben, M. H. M. and De Boer, R. J. 1999. Competition for antigenic sites during T cell proliferation: a mathematical interpretation of *in vitro* data. *Proc. Natl Acad. Sci. USA* 96:10782.

33 Kedl, R. M., Rees, W. A., Hildeman, D. A. *et al.* 2000. T cells compete for access to antigen-bearing antigen-presenting cells. *J. Exp. Med.* 192:1105.

34 Tough, D. F. and Sprent, J. 1994. Turnover of naive- and memory-phenotype T cells. *J. Exp. Med.* 179:1127.

35 Jackola, D. R. and Hallgren, H. M. 1998. Dynamic phenotypic restructuring of the CD4 and CD8 T-cell subsets with age in healthy humans: a compartmental model analysis. *Mech. Ageing Dev.* 105:241.

36 De Boer, R. J., Oprea, M., Antia, R., Murali-Krishna, K., Ahmed, R. and Perelson, A. S. 2001. Recruitment times, proliferation, and apoptosis rates during the CD8$^+$ T-cell response to lymphocytic choriomeningitis virus. *J. Virol.* 75:10663.

37 Jacob, J. and Baltimore, D. 1999. Modelling T-cell memory by genetic marking of memory T cells *in vivo*. *Nature* 399:593.

38 Moskophidis, D., Lechner, F., Pircher, H. and Zinkernagel, R. M. 1993. Virus persistence in acutely infected immunocompetent mice by exhaustion of antiviral cytotoxic effector T cells. *Nature* 362:758.

39 Maile, R., Wang, B., Schooler, W., Meyer, A., Collins, E. J. and Frelinger, J. A. 2001. Antigen-specific modulation of an immune response by *in vivo* administration of soluble MHC class I tetramers. *J. Immunol.* 167:3708.

40 Veiga-Fernandes, H., Walter, U., Bourgeois, C., McLean, A. and Rocha, B. 2000. Response of naive and memory CD8$^+$ T cells to antigen stimulation *in vivo*. *Nat. Immunol.* 1:47.

41 Farber, D. L. 1998. Differential TCR signaling and the generation of memory T cells. *J. Immunol.* 160:535.

42 Welsh, R. M. and McNally, J. M. 1999. Immune deficiency, immune silencing, and clonal exhaustion of T cell responses during viral infections. *Curr. Opin. Microbiol.* 2:382.

43 McKeithan, T. W. 1995. Kinetic proofreading in T-cell receptor signal transduction. *Proc. Natl Acad. Sci. USA* 92:5042.

44 Roncarolo, M.-G. and Levings, M. K. 2000. The role of different subsets of T regulatory cells in controlling autoimmunity. *Curr. Opin. Immunol.* 12:676.

45 Grossman, Z. and Singer, A. 1996. Tuning of activation thresholds explains flexibility in the selection and development of T cells in the thymus. *Proc. Natl Acad. Sci. USA* 93:14747.

46 Bachmann, M. F., Speiser, D. E., Mak, T. W. and Ohashi, P. S. 1999. Absence of co-stimulation and not the intensity of TCR signaling is critical for the induction of T cell unresponsiveness *in vivo*. *Eur. J. Immunol.* 29:2156.

47 Bachmann, M. F., Oxenius, A., Speiser, D. E. *et al.* 1997. Peptide-induced T cell receptor down-regulation on naive T cells predicts agonist/partial agonist properties and strictly correlates with T cell activation. *Eur. J. Immunol.* 27:2195.

48 Rabinowitz, J. D., Beeson, C., Lyons, D. S., Davis, M. M. and McConnell, H. M. 1996. Kinetic discrimination in T-cell activation. *Proc. Natl Acad. Sci. USA* 93:1401.

49 Borghans, J. A. M., Noest, A. J. and De Boer, R. J. 1999. How specific should immunological memory be? *J. Immunol.* 163:569.

50 Lanzavecchia, A., Lezzi, G. and Viola, A. 1999. From TCR engagement to T cell activation: a kinetic view of T cell behavior. *Cell* 96:1.

51 Opferman, J. T., Ober, B. T. and Ashton-Rickardt, P. G. 1999. Linear differentiation of cytotoxic effectors into memory T lymphocytes. *Science* 283:1745.

52 Steinman, R. M. and Nussenzweig, M. C. 2002. Avoiding horror autotoxicus: the importance of dendritic cells in peripheral T cell tolerance. *Proc. Natl Acad. Sci. USA* 99:351.

53 Garza, K. M., Chan, S. M., Suri, R. *et al.* 2000. Role of antigen-presenting cells in mediating tolerance and autoimmunity. *J. Exp. Med.* 191:2021.

54 Noest, A. J. 2000. Designing lymphocyte functional structure for optimal signal detection: *voilà*, T cells. *J. Theor. Biol.* 207:195.

55 Cohen, I. R. 2002. Peptide therapy for type I diabetes: the immunological homunculus and the rationale for vaccination. *Diabetologia* 45:1468.